CEAS Space Journal manuscript No.
(will be inserted by the editor)

Multiple Spacecraft Configuration Designs for Coordinated Flight Missions

Federico Fumenti · **Stephan Theil**

Received: date / Accepted: date

Abstract Coordinated flight allows the replacement of a single monolithic spacecraft with multiple smaller ones, based on the principle of distributed systems. According to the mission objectives and in order to ensure a safe relative motion, constraints on the relative distances need to be satisfied. Initially, differential perturbations are limited by proper orbit design. Then, the induced differential drifts can be properly handled through corrective maneuvers. In this work several designs are surveyed, defining the initial configuration of a group of spacecraft while counteracting the differential perturbations. For each of the investigated designs, focus is placed upon the number of deployable spacecraft and on the possibility to ensure safe relative motion through station keeping of the initial configuration, with particular attention to the required ΔV budget and the constraints violations.

Keywords multiple spacecraft · coordinated flight · station keeping

1 Introduction

In recent years, the interest in spacecraft coordinated flight has increased considerably due to the numerous potential advantages associated with the replacement of a single monolithic object with several smaller ones. A group of small spacecraft working together could enhance scientific observations, augment flexibility and redundancy, reduce costs and risks, and overcome physical limitations. At the same time, however, new challenges are introduced concerning, for example, the sharing of data, the communication, and the relative motion among the objects. Focusing on this last aspect, it is trivial to observe that when multiple objects are considered, careful attention must be paid to the way they move with respect to each other. Constraints may be applied

F. Fumenti
DLR, Institute of Space Systems, Robert Hooke Str. 7, 28359, Bremen
E-mail: federico.fumenti@dlr.de

S. Theil
DLR, Institute of Space Systems, Robert Hooke Str. 7, 28359, Bremen

in order to ensure a safe relative motion and, according to the relative configuration and cooperation among the objects, the two branches of formation flight and cluster flight can be distinguished. Due to many technical limitations the spread of the two architectures did not evolve in the same manner. Consequently, formations are currently a well researched area, whilst work on clusters has so far been lacking.

In a formation of satellites, the relative configuration is fixed and control actions are required to maintain it. In a typical mission scenario, the involved sensors and instruments require an operational distance on the order of hundreds of meters or more, which cannot be achieved using a single spacecraft. The resultant design would not comply with the launch vehicle volume constraints, even if deployment mechanisms were employed. To overcome this issue, the devices can be distributed on different spacecraft which fly together, therefore guaranteeing the satisfaction of the relative distances requirements through the use of control actions. Examples of missions implementing the formation flight concept can be found in TanDEM-X [23], PRISMA [24], and GRACE [29].

In the case of a cluster there is no need for precise geometry, because the successful outcome of the mission does not strictly depend on specific relative configuration as in the formation flight case. As long as the distances among the spacecraft are held within a maximum and a minimum value to ensure inter-module communication and to avoid collisions, respectively, no control action is required. This results in less strict relative motion requirements, and consequently, constraints become more relaxed, as interventions from the control system are less frequent. In a typical scenario each member of the cluster allocates a different functionality, like payloads, communications, data storage, etc. and all the functionalities are shared through wireless connections. Examples for potential application of the cluster flight can be identified in the missions PLEIADES [18] and SAMSON [16].

In the design of a coordinated spacecraft-based mission, an extremely important task is the definition of the initial configuration, since the application of proper constraints on the relative states will induce a particular desired behavior in the evolution of the relative motion. Over time corrective maneuvers are required to counteract the changes in the initial relative geometry deriving from the differential perturbations. Therefore, to limit the required fuel and the missions costs, it is highly desirable to have orbits that naturally satisfy the relative motion constraints. Over the years many authors have worked on the development and improvement of mathematical models in order to grasp the evolution of the relative motion and simplify the application of the required constraints (see e.g., [7, 8, 17, 19, 20, 28, 30, 34]).

Once the initial configuration is defined and the spacecraft are deployed, a station keeping approach could be used to cancel the drifts induced by differential perturbations. Indeed, the initial states ensure satisfaction of the distance constraints and can be considered reference states to be tracked. This approach is certainly meaningful in a formation, where the relative geometry constraints considerably limit the tolerable differential drifts. Perhaps less clear is the benefit posed by station keeping in a cluster scenario. In this case the loose constraints imply that the distance boundaries are infrequently violated and when this happens the drift from the reference state could be so large that the recomputation of a new reference state could become more meaningful than the station keeping of the old one. The goal of this work is to evaluate

if and if so, by how much the station keeping logic could be beneficial for coordinated flight missions characterized by a different number of spacecraft and different distance boundaries. To study and implement the station keeping logic, it can be advantageous to express the relative motion through relative orbital elements, since the variation over time of the orbital elements is much smaller than that of the Cartesian coordinates. In addition, corrections of specific elements with theoretically no effect on the others can be obtained using impulsive control (see e.g., [4, 14, 21, 25–28]).

According to the type of constraints initially imposed, various initial configurations can be found, differing from each other by the number of deployable spacecraft, their relative geometry and the effort, in terms of ΔV, they require for station keeping. A survey and comparison of such initial configurations is the topic of this paper, which extends the work of Fumenti and Theil [15] and is organized as follows. Section 2 introduces the problem and the techniques used to define the initial states of a group of spacecraft. Section 3 describes how the comparison has been established, along with the key parameters used, and presents the results of the study. Section 4 reports the final conclusions.

2 Problem Statement

The successful outcome of a coordinated flight-based mission strictly depends on the relative motion among the involved spacecraft. To ensure satisfaction of relative motion constraints, much attention must be paid in terms of control actions to counteract differential perturbations. In order to reduce the fuel expenditure, specific constraints can be imposed in the definition of the initial conditions according to the desired behavior, which is dictated by the mission objectives.

From the literature research it emerged that several techniques used to define the relative initial conditions of a group of satellites are available, hence it has been decided to examine and compare them, to determine if and how the computed initial conditions could be used for the deployment of a cluster of objects.

The techniques for the definition of the initial conditions (TIC) that have been studied are introduced in the upcoming sections but first, in order to make their comparison meaningful, a common test setup with the following features is identified:

- the cluster is centered on a virtual point (VP), which is mass-less and moves on a Low Earth Orbit (LEO); its state at the initial time t_0 is defined in Table 1 in terms of osculating keplerian elements $\mathbf{oe}^K_{VP}(t_0) = (a \;\; e \;\; i \;\; \omega \;\; \Omega \;\; M)^T$.
- a minimum distance D_{min} must be ensured between any pair of spacecraft to prevent collisions
- a maximum distance D_{max} must be ensured between any spacecraft and the VP to prevent escaping drifts.

Let us denote with d_s and d_r the generic distances between any two spacecraft of the cluster and between a spacecraft and the VP, respectively. The minimum and the maximum distance constraints are given by:

$$d_s \geq D_{min} \tag{1a}$$

$$d_r \leq D_{max}. \tag{1b}$$

Element	Value	Units
semi-major axis - a	7000.92	km
eccentricity - e	0.01	
inclination - i	50.99	deg
right ascension of the ascending node - Ω	11.48	deg
argument of perigee - ω	19.12	deg
mean anomaly - M	21.00	deg

Table 1 Initial state of the virtual point.

Although the reason for limiting the distances d_s should be trivial, the use of a virtual point and the application of the maximum distance constraint to the distances d_r might be unclear. To ensure that the spacecraft do not drift apart and the cluster does not disintegrate, instinctively one would upper bound the distances d_s and properly adapt Eq. (1b). The use of the virtual point, however, brings some interesting advantages, such as the opportunity to have direct information about the nominal behavior of the cluster and, computationally speaking, the reduction of the number of constraints used in the definition of the cluster configurations, since only one constraint of type Eq. (1b) is required for each spacecraft.

The description of each technique is structured in two parts. First the basic logic is introduced while using the simple chief-deputy framework. The chief is the virtual point and the state of the deputy is defined such that their relative distance is bounded by D_{min} and D_{max}. Afterwards, it is shown how the same logic can be adapted to configure a cluster of n_m modules while also maximizing n_m. Indeed, for cluster flight the chief-deputy approach does not fit very well as it is, and for several reasons. In the first place, from the stated assumptions it is clear that there is no need to lower bound the distances d_r and to upper bound the distances d_s. Secondly, when several modules are placed into the cluster and the chief-deputy technique is applied to every module, information about the motion of the spacecraft with respect to the VP is available, but nothing can be said about a deputy-deputy type of motion. Plus, the idea of studying the motion of each agent with respect to all the others is inconceivable, since as n_m grows the problem quickly becomes extremely complex and unmanageable (for a given n_m the number of pairs to be considered is in fact equal to $0.5n_m(n_m-1)$).

After a brief introduction of the different techniques, a comparison of their performances will be discussed. Results based on their application to the obtainment of clusters of different sizes will be presented while focusing on the features of capacity, i.e. how many spacecraft can populate the clusters, and of consumption, i.e. how much ΔV is required for cluster keeping. In order to establish a meaningful comparison, a simple and uniform metric is applied to all the techniques: each spacecraft tracks a reference spot and cluster keeping is investigated through station keeping.

In order to clarify the descriptions of the investigated techniques in the upcoming sections, the distinction between keplerian and non-singular orbital elements is briefly revised here, since both of them will be used. The keplerian set of elements $\mathbf{oe}^K$ has been actually already introduced through Table 1, while the non-singular set is given by $\mathbf{oe}^N = (a \;\; u \;\; e_x \;\; e_y \;\; i \;\; \Omega)^T$, where $e_x = e\cos\omega$ and $e_y = e\sin\omega$ are the com-

ponents of the eccentricity vector $\mathbf{E} = (e_x\ e_y)^T$ and $u = \omega + M$ is the mean argument of latitude. In addition, it is worth recalling that when two spacecraft are considered and their states are expressed in terms of orbital elements, the relative motion of the deputy D with respect to the chief C can be expressed in terms of relative orbital elements. In the keplerian case, given the vectors $\mathfrak{oe}_C^K$ and $\mathfrak{oe}_D^K$, the relative elements are simply computed as the difference between the elements of the two objects:

$$\Delta\mathfrak{oe}^K = \mathfrak{oe}_D^K - \mathfrak{oe}_C^K = (\Delta a\ \ \Delta e\ \ \Delta i\ \ \Delta\Omega\ \ \Delta\omega\ \ \Delta M)^T. \tag{2}$$

In the non-singular case, the vectors $\mathfrak{oe}_C^N$ and $\mathfrak{oe}_D^N$ lead to the relative elements through a nonlinear combination:

$$\begin{aligned}\Delta\mathfrak{oe}^N &= \begin{pmatrix} \Delta\widetilde{a} & \Delta\lambda & \Delta e_x & \Delta e_y & \Delta i_x & \Delta i_y \end{pmatrix}^T \\ &= \begin{pmatrix} \Delta a/a & \Delta u + \Delta\Omega\cos i & \Delta e_x & \Delta e_y & \Delta i & \Delta\Omega\sin i \end{pmatrix}^T\end{aligned} \tag{3}$$

where $\Delta\widetilde{a}$ is an additional measure of the differential semi-major axis, $\Delta\lambda$ is the differential mean longitude, Δe_x and Δe_y are the components of the relative eccentricity vector $\Delta\mathbf{E} = (\Delta e_x\ \Delta e_y)^T$, and finally Δi_x and Δi_y are the components of the relative inclination vector $\Delta\mathbf{I} = (\Delta i_x\ \Delta i_y)^T$.

2.1 Eccentricity/Inclination Vector Separation Technique

The Eccentricity/Inclination (E/I) vector separation technique (EIVS) is particularly attractive since it can naturally enforce collision avoidance. It has been originally proposed to face the problem of satellites colocation in geostationary slots [13] and in the last years widely investigated and successfully applied also for formations of satellites in LEO ([9, 10, 22]).

To better observe the relative orbit, a rotating reference frame as shown in Fig. 1 can be introduced. This is known as the local vertical local horizontal (LVLH) frame and has the origin coincident with the chief spacecraft C, while the $r\theta$-plane is assumed to lie on its orbital plane with the r-axis parallel to its position vector (positive outwards).

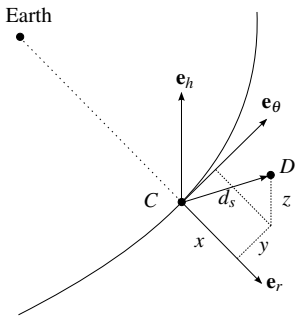

Fig. 1 LVLH reference frame.

Through the use of the LVLH frame, the relative motion can be expressed in non-dimensional form through:

$$\frac{x}{a} = \delta x(u) \approx \ \Delta\widetilde{a} \qquad -\Delta E\cos(u-\vartheta) \tag{4a}$$

$$\frac{y}{a} = \delta y(u) \approx \ -\frac{3}{2}\Delta\widetilde{a}u + \Delta\lambda \quad +2\Delta E\sin(u-\vartheta) \tag{4b}$$

$$\frac{z}{a} = \delta z(u) \approx \qquad +\Delta I\sin(u-\varphi) \tag{4c}$$

where $\Delta\mathbf{E}$ and $\Delta\mathbf{I}$ are expressed in polar notation, with $\Delta E = \|\Delta\mathbf{E}\|$ and $\Delta I = \|\Delta\mathbf{I}\|$, and with ϑ and φ being the relative perigee and the relative ascending node [9]. An overview of the relative motion as described by Eq. (4) is given in Fig. 2.

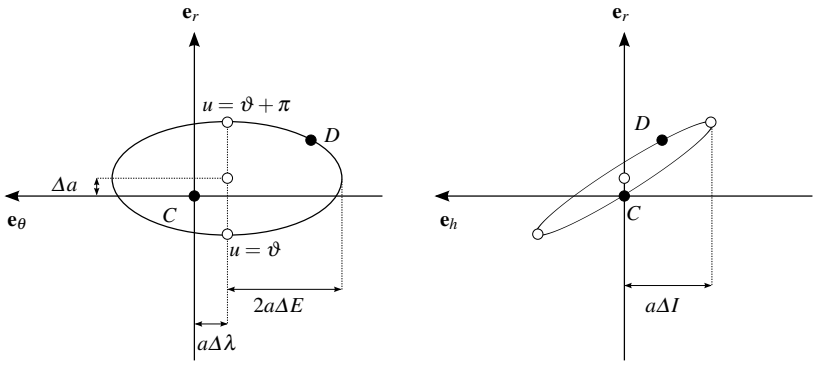

Fig. 2 Relative motion described by relative eccentricity and inclination vectors. Projections of the relative orbit on *xy*-plane (left) and *zx*-plane (right).

Assuming $\Delta\lambda = 0$ and $\Delta a = 0$ to cancel the offsets and to prevent the drift in the along-track direction, the collision risks can be reduced by setting:

$$\vartheta \ = \varphi + k\pi \tag{5a}$$

$$D_{min} \ \leq a\min\{\Delta E, \Delta I\} \tag{5b}$$

with integer k, while the constraint

$$a\sqrt{4\Delta E^2 + \Delta I^2} \leq D_{max} \tag{6}$$

ensures satisfaction of the maximum distance constraint. In particular, Eq. (5a) represents the so-called (anti-)parallelism condition, which not only ensures that the radial and the cross-track distances never vanish together, but also that when one of them is zero, the other assumes its maximum value, so that even in the presence of position uncertainties in the along-track direction, the risks of collisions are minimized. Equations (5b) and (6) permit instead to define the magnitude of the E/I relative vectors, such that the relative orbit respects the minimum and maximum distances. If the J_2 perturbation is included in the model represented by Eq. (4), $\Delta a = 0$ is not valid anymore and Eqs. (5) and (6) need to be adapted [9].

To better relate the E/I relative vectors with the distances, it could be useful to consider their dimensional version obtained by multiplying them by the semi-major axis of the VP. The new dimensional parameters can be distinguished from the original ones by the presence of a small hat ($\widehat{\ }$), so that $\Delta\widehat{E} = a\Delta E$, $\Delta\widehat{I} = a\Delta I$ and so on. Then, in the design phase, it can be helpful to define the elements of the spacecraft in the planes $\Delta\widehat{e}_x\Delta\widehat{e}_y$ and $\Delta\widehat{i}_x\Delta\widehat{i}_y$.

Let us now see how the EIVS approach can be used to configure a cluster with multiple objects. The problem can be geometrically approached in two steps:

1. in each of the two planes $\Delta\widehat{e}_x\Delta\widehat{e}_y$ and $\Delta\widehat{i}_x\Delta\widehat{i}_y$, the D_{max} is used to identify a region around the origin, which includes points satisfying the maximum distance constraint;
2. in each region, points are chosen with a mutual distance at least equal to D_{min}.

An example of how the described geometric logic can be applied is given in Fig. 3, where each point represents the relative eccentricity (left plot) and the relative inclination (right plot) vector of a spacecraft with respect to the VP, which is highlighted as a small circle at the origin of the planes.

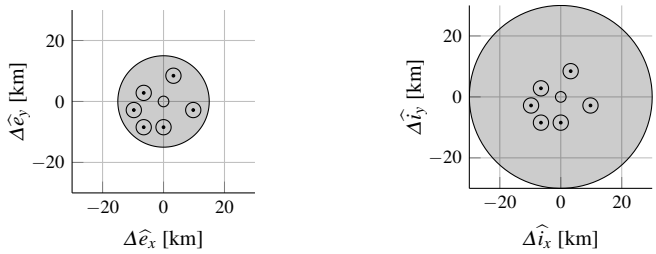

Fig. 3 Example of relative eccentricity (left) and inclination (right) vectors for a cluster of 6 spacecraft.

Provided that in each plane every point is sufficiently spaced from all the others and that corresponding points from the two planes satisfy the (anti-)parallelism condition (Eq. (5a)), the satisfaction of the minimum distance can be ensured. In the given example, the minimum distance constraint is based on a value $D_{min} = 5$ km and is represented by the small circles. The fulfillment of the maximum distance constraint can instead be studied by taking into consideration the distance of the points from the origin of the planes. These constraints are based on a value $D_{max} = 30$ km and are represented by the gray regions, which can be evaluated through Eq. (4). It can be noted that in Fig. 3 corresponding points from the two planes, do not only share the same phase of the relative vectors, but also have the same magnitude. This is the reason why in the right plot of Fig. 3 the points are concentrated in the center, leaving the outer part of the gray region empty. The condition of equal magnitudes is not required by the EIVS technique, but it has been introduced to limit the differential perturbations experienced by the spacecraft.

With the above-mentioned example it has been shown how the selection of the relative E/I vectors can be performed while using simple 2-D geometry. Six points

have been chosen from the gray regions, but this number can easily grow if a smarter selection is performed and the points are taken, for example, from a regular grid. The maximization of the spacecraft number n_m therefore becomes a packing problem, since it turns into the research of the maximum number of points that can be placed into a given 2-D region. In this study three regular grids have been considered to place the points in the two planes and they are shown in Figs. 4(a) to 4(c).

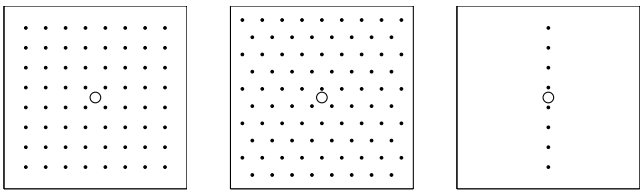

(a) Grid N.1 (b) Grid N.2 (c) Grid N.3

Fig. 4 Regular grids for the 2-D packing problem of the EIVS technique.

The grid in Fig. 4(a) is obtained through a square packing, where each point and the eight surrounding it are located at the center and on the perimeter of a square, respectively. In a similar way, Fig. 4(b) gives an example of a hexagonal packing, since each point occupies the center of a regular hexagon and is surrounded by six points located at the vertices of the hexagon. To conclude, the grid presented in Fig. 4(c) is simply a particular example of the square packing case.

For the evaluation of the number of points, clearly the first and the second grid should be preferred over the third one. In most of the cases the highest number of points is obtained with the second grid, but according to the size of the 2-D region, there are a few cases where the first grid performs better. The third grid returns a number of points much smaller than the others, but it has been included in the study, as it is perhaps promising for the analysis of the corrective maneuvers, which will be presented in the following sections. To properly understand the interest in the Grid N.3, let us apply it on the $\Delta\widehat{i}_x\Delta\widehat{i}_y$ plane for the definition of the relative inclination vectors. The fact that all the points belong to the y-axis leads easily to the result that all the obtained state vectors have the same inclination. Less intuitive is instead the result that also the semi-major axes are all the same, due to the tight connection between the differential inclination and the differential semi-major axis [9]. The absence of a differential semi-major axis limits considerably the effect of differential perturbations, with the consequence that the fuel consumption required to cancel the experienced drifts should be much smaller than that associated with state vectors obtained from the first or the second grid.

2.2 J_2 Invariance Technique

The technique of the J_2 invariance (J2In) consists in placing the spacecraft in orbits for which the relative drift is minimized [1, 26]. To focus on the long term behavior,

the mean orbital elements $\overline{\mathbf{oe}}^K$ are used, with Eq. (7) showing the effect of the J_2 perturbation on their evolution [3]:

$$\frac{d\overline{\Omega}}{dt} = -\frac{3}{2}J_2\overline{n}\left(\frac{R_E}{\overline{p}}\right)^2\cos\overline{i} \tag{7a}$$

$$\frac{d\overline{\omega}}{dt} = -\frac{3}{4}J_2\overline{n}\left(\frac{R_E}{\overline{p}}\right)^2\left(5\cos^2\overline{i}-1\right) \tag{7b}$$

$$\frac{d\overline{M}}{dt} = \overline{n}+\frac{3}{4}J_2\overline{n}\left(\frac{R_E}{\overline{p}}\right)^2\sqrt{1-\overline{e}^2}\left(3\cos^2\overline{i}-1\right). \tag{7c}$$

where $\overline{n}=\sqrt{\mu/\overline{a}^3}$ and $\overline{p}=\overline{a}\sqrt{1-\overline{e}^2}$ are the mean mean motion and the mean semi-latus rectum of the VP, while μ and R_E are the gravitational parameter and the radius of the Earth. It can be noted that the J_2 term only alters the elements $[\overline{\Omega}\ \overline{\omega}\ \overline{M}]$ and that these elements only depend on the remaining elements $[\overline{a}\ \overline{e}\ \overline{i}]$ (the elements $[\overline{a}\ \overline{e}\ \overline{i}]$ remain instead constant, which is why their rates are omitted in Eq. (7)). Therefore, the minimization of the spacecraft relative drift must be sought by selecting proper sets of $[\overline{a}\ \overline{e}\ \overline{i}]$ that match the rates of variation of $[\overline{\Omega}\ \overline{\omega}\ \overline{M}]$.

Several strategies can be followed to perform the matching process [1, 26]. For example, instead of focusing on the rates $[\dot{\overline{\Omega}}\ \dot{\overline{\omega}}\ \dot{\overline{M}}]$, one can decide to combine them in order to cancel other kinds of drifts, such as the drift in the argument of latitude, or the drift in the along-track direction. In this paper, the approach from Schaub and Alfriend [26] is used, which aims at minimizing the drift in the ascending node and in the argument of latitude. The constraints are expressed in terms of the deputy relative elements, hence the following expressions can be retrieved:

$$\eta\Delta\overline{a}+2D\overline{ae}\Delta\overline{e}=0 \tag{8a}$$

$$\eta^2\tan\overline{i}\Delta\overline{i}-4\overline{e}\Delta\overline{e}=0 \tag{8b}$$

where the absolute and differential elements used are the ones of the chief and of the deputy, respectively. In addition, $\eta=\sqrt{1-\overline{e}^2}$, $D=\frac{J_2}{4L^4\eta^5}(4+3\eta)(1+5\cos^2\overline{i})$ and $L=\sqrt{\overline{a}/R_e}$ hold. Note that Eq. (8) allows for conputation of $\Delta\overline{a}$ and $\Delta\overline{i}$ when $\Delta\overline{e}$ is fixed, but it also remains valid if $\Delta\overline{a}$ or $\Delta\overline{i}$ are given. Finally, in concerns to the remaining differential elements $[\Delta\overline{\Omega}\ \Delta\overline{\omega}\ \Delta\overline{M}]$, they can be freely chosen as long as they satisfy all the constraints on the relative distances.

Let us now approach the problem for the cluster case. If multiple objects are involved in the process, the J_2 invariance should be ensured for all of them, meaning that the relative orbit between any pair of objects should be J_2 invariant. In this perspective Eq. (8) should be applied for each pair of elements (sat/VP and sat/sat), thus turning into a set of $2n_p$ conditions, with $n_p=0.5n_m(n_m+1)$ denoting the number of the pairs. As soon as $n_m>2$ the system becomes over-determined and needs then to be solved numerically, and so it becomes useful recasting Eq. (8) into the form

$$|\eta\Delta\overline{a}+2D\overline{ae}\Delta\overline{e}|<\varepsilon \tag{9a}$$

$$|\eta^2\tan\overline{i}\Delta\overline{i}-4\overline{e}\Delta\overline{e}|<\varepsilon \tag{9b}$$

where ε is a user-defined threshold within which the solution must satisfy the constraints. According to the approximations used in the derivation of Eq. (8) (only terms of $\mathscr{O}(J_2)$ have been retained) [26], in the performed study it has been assumed $\varepsilon = 10^{-3}$, in order to have the same order of magnitude of the J_2 coefficient.

The next step towards the definition of a cluster configuration consists in identifying the range of values from which the parameters $\Delta\overline{a}$, $\Delta\overline{e}$, and $\Delta\overline{i}$ can be chosen.

Given two objects A and B and assuming that their relative orbits are J_2 invariant, it should be implied that the relative orbit of A with respect to B, as well as the relative orbit of B with respect to A, is invariant. It should not matter which object is the chief and which is the deputy. Mathematically speaking Eq. (9) must hold both when it uses the orbital elements of A with the relative elements of B with respect to A, and when it uses the orbital elements of B with the relative elements of A with respect to B. In this paper this condition has been called *double invariance* and particular attention has been placed on it, as it has been noted that this condition is not fulfilled if the differential elements $[\Delta\overline{a}\ \Delta\overline{e}\ \Delta\overline{i}]$ are too large. There are cases in which the elements of B are selected to ensure that its relative orbit with respect to A is J_2 invariant, but then inverting the roles and checking the relative orbit of A with respect to B, the J_2 invariance constraints are violated.

To avoid this situation, the ranges of the differential elements which are able to ensure the desired double invariance have been researched. According to the eccentricity of the VP, the attention has been focused on the interval $-0.009 < \Delta\overline{e} < 0.039$, which has then been divided into a regular grid. For all grid points the double invari-

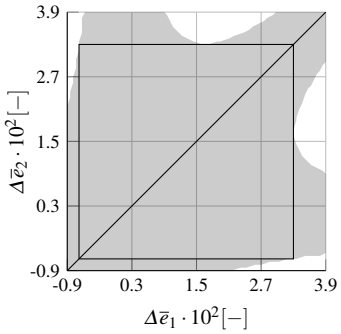

Fig. 5 Map of the J_2 double invariance shown in terms of relative eccentricities.

ance has been pairwise checked and the results are depicted in Fig. 5. The gray area emphasizes the satisfaction of the double invariance, which for example, is fulfilled by two objects which have orbital elements defined with differential eccentricities equal to 2.7×10^{-2} and -0.3×10^{-2}, but not for those two with orbital elements obtained from the values 3.9×10^{-2} and 1.5×10^{-2}. Note that the plot is symmetric with respect to the plane bisector and therefore for both given examples, the results do not depend on the assignment of values to objects. Finally the black-sided square highlights the desired range for the differential eccentricity, so that if all the relative orbits of the cluster satisfy

$$\begin{array}{ccccc} -0.023 \text{ km} & < & \Delta\bar{a} & < & 0.048 \text{ km} \\ -0.007 & < & \Delta\bar{e} & < & 0.033 \\ -0.00025 \text{ rad} & < & \Delta\bar{i} & < & 0.00120 \text{ rad} \end{array} \tag{10}$$

they are all J_2 invariant with respect to each other. In Eq. (10) the range of $\Delta\bar{e}$ comes directly from Fig. 5, while the ranges for $\Delta\bar{a}$ and $\Delta\bar{i}$ can be easily computed through Eq. (8).

To investigate the cluster case, the definition of the initial configuration can be expressed as the determination of those vectors $\Delta\overline{\mathbf{oe}}_i^K$ (with $i = 1,2,...,n_m$), whose elements are bounded by the conditions given in Eq. (10) and at the same time fulfill a system of nonlinear conditions given by the $2n_p$ equations obtainable from Eq. (8) and by additional equations deriving from the application of Eq. (1).

In the way the problem has been described and implemented, it is trivial that n_m is not a variable, but a parameter provided by the user. Therefore, to maximize the number of spacecraft n_m that the cluster can allocate, the problem can be solved heuristically, by searching for optimal solutions while using different values of n_m. The search process starts with a low n_m, and constantly increases it, as long as an optimal solution can be obtained. The search is over and the maximum n_m is detected when the problem becomes infeasible and no solutions can be found anymore.

2.3 Distance Bounded Natural Orbits Technique

The technique of the distance-bounded natural orbits (DBNO), as suggested by the name itself, aims at finding orbits that naturally satisfy the distance constraints. The technique is presented in Mazal and Gurfil [19] and relies on a constraint which is proven to ensure bounded relative distances when a time invariance assumption for the environmental perturbations is made. This idea is similar to the J2In approach, but this time the invariance can take all perturbations imposed by the gravitational potential into account.

As proven in [19], given two objects A and B with equal ballistic coefficients, if

$$\text{œ}_B(t_0) = \text{œ}_A(t_0) + \int_{t_0}^{t_0+\Delta t} \dot{\text{œ}}_A dt + [0\ 0\ 0\ \Delta\Omega\ 0\ 0]^T \tag{11}$$

then the following condition holds

$$2\gamma_{min} \sin\left(\frac{|\Delta\Omega|}{2}\right) - V_{max}|\Delta t| \leq d_s(t) \leq 2\gamma_{max} \sin\left(\frac{|\Delta\Omega|}{2}\right) + V_{max}|\Delta t| \tag{12}$$

where V_{max} denotes the maximum speed of A, while γ_{max} and γ_{min} denote its maximum and minimum equatorial projections. It holds indeed $\gamma_A(t) = \sqrt{X_A^2(t) + Y_A^2(t)}$, with X and Y components of the position vector in an inertial frame.

For a given set of constraints on the minimum and maximum distances D_{min} and D_{max}, the values Δt and $\Delta\Omega$ can be chosen while satisfying

$$2\gamma_{min}\sin\left(\frac{|\Delta\Omega|}{2}\right) - V_{max}|\Delta t| \geq D_{min} \tag{13a}$$

$$2\gamma_{max}\sin\left(\frac{|\Delta\Omega|}{2}\right) + V_{max}|\Delta t| \leq D_{max} \tag{13b}$$

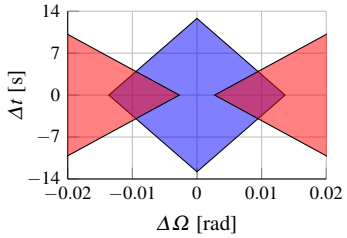

Fig. 6 Example of Δt and $\Delta\Omega$ selection while satisfying the constraints on the minimum distance ( ) and on the maximum distance ( ).

Equation (13) can be observed graphically in Fig. 6, showing for which values of $\Delta\Omega$ and Δt the distance constraints are satisfied, when $D_{min} = 5$ km and $D_{max} = 100$ km are considered. The satisfaction of each constraint is highlighted with a different color and therefore for the mission design a pair $[\Delta\Omega\ \Delta t]$ must be selected from the overlapping area.

In the case of n_m spacecraft, the DBNO technique retains validity as long as the constraints expressed through Eq. (13) are applied to each pair. The differences in time and right ascension of the ascending node (RAAN) of the i-th spacecraft with respect to the VP can be denoted as $\Delta\Omega_{0i}$ and Δt_{0i}, while the differences between any pair of spacecraft $(i,\ j)$ can be denoted as

$$\begin{cases} \Delta\Omega_{ij} = \Delta\Omega_{0j} - \Delta\Omega_{0i} \\ \Delta t_{ij} = \Delta t_{0j} - \Delta t_{0i} \end{cases} \qquad \text{with } i,j = 1,2,...,n_m \text{ and } j \neq i. \tag{14}$$

In addition, the small angles approximation can be introduced to replace the sine functions with their arguments. In this work several D_{max} up to few hundreds of km will be considered, leading to a maximum differential RAAN of few degrees totally compatible with this approximation. Equation (13) then turns into:

$$\gamma_{min}|\Delta\Omega_{ij}| - V_{max}|\Delta t_{ij}| \geq D_{min} \tag{15a}$$

$$\gamma_{max}|\Delta\Omega_{0i}| + V_{max}|\Delta t_{0i}| \leq D_{max}. \tag{15b}$$

It is worth noticing that for the current study the assumptions required by the DBNO technique do not entirely hold, because in its original formulation the technique requires the equality of the ballistic coefficients, while in the considered scenario the VP is a mass-less point. This means that if the environmental model includes the

atmospheric drag, the satisfaction of Eq. (15b) will still ensure a substantial reduction of the differential perturbation between a spacecraft and the VP, however, the drifts in their relative motion will be larger than the ones predicted by the original formulation.

When approaching the problem while trying to maximize the number of modules n_m, Eq. (15b) is immediately used to define the domain of the differential time and RAAN from which the sets $[\Delta\Omega_{0i}\ \Delta t_{0i}]$ should be selected. On the other hand, Eq. (15a) is exploited for the actual selection of the sets $[\Delta\Omega_{0i}\ \Delta t_{0i}]$. From a first glimpse at Eq. (15a) and with the help of Fig. 6, it can be seen that it is never possible to satisfy the minimum distance constraint with a pure time shift and that a minimum differential RAAN $|\Delta\Omega|_{min}$ is always required. Indeed, exploiting Eq. (15a) and the fact that $|\Delta t_{ij}| > 0$, the minimum value $|\Delta\Omega|_{min}$ can be retrieved

$$|\Delta\Omega_{ij}| > \frac{D_{min}}{\gamma_{min}} \equiv |\Delta\Omega|_{min} \tag{16}$$

and the differential RAAN can be chosen according to $|\Delta\Omega_{ij}| = (1+k_\Omega)|\Delta\Omega|_{min}$ with a small $k_\Omega > 0$. In turn an upper bound for the time shift can be defined as

$$|\Delta t_{ij}| < \frac{k_\Omega D_{min}}{V_{max}} \equiv |\Delta t|_{max} \tag{17}$$

and similarly to what has been set for the differential RAAN, the differential times can be chosen according to $|\Delta t_{ij}| = (1-k_t)|\Delta t|_{max}$ with a small $k_t > 0$. It is worth noting that the determination of the two boundaries $|\Delta\Omega|_{min}$ and $|\Delta t|_{max}$ and the selection of the two coefficients k_Ω and k_t do not depend on the specific pair $(i,\ j)$, therefore it is possible to define the values of the four parameters just once and subsequently use them to find the initial condition of all the spacecraft.

At this point, it is clear that dividing the $\Delta\Omega$ domain into a grid of points equally spaced by $(1+k_\Omega)|\Delta\Omega|_{min}$ facilitates the definition of the differential RAAN $\Delta\Omega_{0i}$ and the maximization of the number of spacecraft n_m at the same time. Concerning the time shifts, a trivial solution can be obtained assuming $\Delta t_{0i} = 0\ \forall i$. Otherwise, if time shifts different from zero are desired, they can be selected through the knowledge of the $|\Delta t|_{max}$.

2.4 Delayed Elements Technique

The technique of the delayed elements (DeEl) is very similar to the DBNO technique, since it aims at finding relative orbits which are invariant with respect to the perturbations deriving from the full gravitational potential. The main difference consists in the fact that the elements of the spacecraft in this case are obtained only through the use of the time difference Δt, which means that all the members of the cluster pass through the same positions of the virtual point, but with a time difference Δt [11]. In this way, all the spacecraft experience the same perturbations with minimal variations from the gravitational field and with the consequence that maneuvers to counteract differential perturbations are greatly reduced.

The cluster obtainable with this technique can be imagined as a train of spacecraft separated in the along-track direction, just like pearls on a string. Reference to separation distance d or time difference Δt is equivalent, since these two quantities can be easily related by exploiting the knowledge of the mean motion. Indeed, given a spacecraft with mean motion n moving for a time Δt, the distance d between the initial and the final positions can be approximated with the traveled arc of trajectory $\widehat{d}$, which exploiting Kepler's second law can be expressed as

$$\widehat{d} = \frac{abn\Delta t}{r} \tag{18}$$

where b is the semi-minor axis of the orbit and r is the position vector magnitude. It is worth noticing that on an elliptical orbit r changes with time; thus, according to the location of the spacecraft along the orbit, a different $\widehat{d}$ can correspond to the same Δt. For this reason, as soon as the maximum and the minimum values of r are computed, the minimum and the maximum distances corresponding to the given Δt are also known. From a different point of view, when the D_{min} and D_{max} values are given, the evaluation of the required time difference Δt is straightforward. This is exactly how the initial conditions of two spacecraft can be defined, since in this case the D_{min} and D_{max} are assumed to be known and can be used to retrieve a range of values from which the Δt should be picked to satisfy the distance constraints. After the Δt is chosen, the initial state of a spacecraft B can be computed from the state of a spacecraft A through Eq. (11), assuming $\Delta\Omega = 0$.

In a similar way, the configuration of an entire cluster can be approached, with the core of the process consisting in the identification of the time shifts associated with the different objects of the cluster. From this perspective, following the example of the DBNO technique, it can be useful to distinguish between the time shifts of the spacecraft with respect to the VP Δt_{0i} and the time shifts among the spacecraft

$$\Delta t_{ij} = \Delta t_{0j} - \Delta t_{0i} \tag{19}$$

with $i, j = 1, 2, ..., n_m$ and $i \neq j$. The constraints on the distances only appear indirectly, in as much as they are used to define an upper and a lower bound for the values of the time shifts Δt_{0i}, which need to be researched while satisfying Eq. (19). In particular, the constraint on the maximum distance defines the maximum allowed time shift $|\Delta t|_{max}$ of a spacecraft with respect to the VP, meaning that it should result in $\frac{\Delta t_{0i}}{|\Delta t|_{max}} \in [-1\ 1]$. On the other hand, the minimum distance constraint is taken into account computing the minimum time shift $|\Delta t|_{min}$ that corresponds to the minimum distance D_{min}, and ensuring that $|\Delta t_{ij}| > |\Delta t|_{min}\ \forall(i, j)$.

Finally, when the interval $[-|\Delta t|_{max}\ |\Delta t|_{max}]$ is divided into sub-intervals of length $|\Delta t|_{min}$, the problem of maximizing the number of spacecraft n_m is also addressed, with the nodes of the grid denoting the time shifts Δt_{0i}.

2.5 Brute Force Packing Technique

The last technique examined is based on brute force to pack the maximum number of objects inside a fixed volume of space, thus the acronym BFPa has been used.

The packing logic is similar to the one used for the grids in the EIVS technique, being that the goal is the maximization of the number of spacecraft while keeping them at a mutual distance at least equal to D_{min}. Nevertheless, the problem must now be formulated in three dimensions. Indeed, in the EIVS case the points represent mathematical quantities and have to be packed in a 2-D region, while this time they represent positions in 3-D space.

From the EIVS section the arrangements of the points within a plane are already known, and for the BFPa technique the first and the second grid can be recycled. Additional investigation is instead required for the arrangement of the planes in the third direction, since no information was available from the previously considered techniques. The simplest solution consists in stacking on top of each other planes of points of the same type, leading to a structure that can be denoted as simple vertical stacking. In addition, since the packing problem is well-known in mathematics, it has been deemed appropriate to use the regular arrangements known as cubic close packing [31] and hexagonal close packing [32]. An overview of how the described arrangements are built is given in Fig. 7.

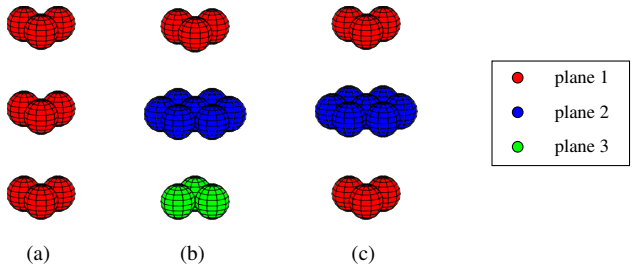

Fig. 7 Regular arrangements for close packing of spheres in a 3-D region: a) simple vertical stacking b) cubic close packing c) hexagonal close packing

The knowledge of the parameter D_{max} can be easily exploited to compute the volume around the VP accessible by the spacecraft. Then, applying to this region of space the regular arrangements previously introduced, the positions of the spacecraft are identified in the LVLH frame. By construction of the grid, those positions ensure the satisfaction of the constraints at the initial time t_0 but nothing can be said about the evolution of the relative motion. To see what happens for $t > t_0$, one should propagate the initial state for each spacecraft, compute all the relative distances and check if the distance constraints hold. In this way, the spacecraft that violate the constraints can be discarded and a safe cluster can be identified.

To perform the propagation of the initial states it is first required to finish forming the initial states themselves, given that so far only the positions are known, while the velocities are still to be determined. For each point of the grid the velocity components in the x and y direction can be computed through:

$$2\dot{x} + ny = 0 \tag{20a}$$

$$\dot{y} + 2nx = 0 \tag{20b}$$

which play the role of constraints required to ensure closed relative motion, as it can be recovered from Eq. (4) or from the classical definition of the cartesian relative motion in the Hill frame [5]. It is worth pointing out that while it is fundamental to minimize the drifts in the along-track direction (Eq. (20b)), it is not strictly necessary to have relative orbits centered on the virtual point (Eq. (20a)). The use of Eq. (20a) represents a tradeoff between the computational effort and the size of the state space, since it allows the reduction of the domain for the search of the velocity components. No information is in fact available for the computation of the third component $\dot{z}$, which is totally free and has to be necessarily explored in a brute force manner. By constraining the $\dot{x}$, one can already determine two out of three components of the velocity vector and thus, the brute force has to deal only with one parameter.

Due to the weak conditions imposed to limit the differential perturbations, the BFPa technique is not expected to be fuel friendly, since the spacecraft drift very fast from/into each other and a considerable amount of maneuvers is required to keep the distance constraints satisfied. The advantage of this technique is in the cluster capacity, since the poor constraints should be able to provide configurations of clusters populated by a large number of objects.

3 Comparison of the Techniques

To analyze the behavior of the different techniques and perform an effective comparison, the number of spacecraft populating the cluster and the ΔV they require for the corrective maneuvers have been considered.

The maximum number of points n_m that can be packed into a given volume of space around the VP clearly depends on the distance constraints, since for a given value of D_{min} an increase of D_{max} involves a larger volume around the VP with the opportunity to allocate more points in it, while for a given value of D_{max} an increase of D_{min} involves a larger safety distance between any pair of points with a consequent reduction of their total number for that same volume. This makes n_m dependent on three different aspects of the problem: the TIC, the D_{min}, and the D_{max}. To observe the effect of the distances, the constraints given in Eq. (1) have been applied with several values of D_{min} and D_{max}. For the sake of brevity, in the following a specific set of values $[D_{min}\ D_{max}]$ is denoted as $D_R = D_{min}/D_{max}$ so that, for example, the notation $D_R = 1/10$ indicates that the cluster needs to satisfy a $D_{min} = 1$ km and a $D_{max} = 10$ km.

Concerning the ΔV, it is clear that due to the differential perturbations experienced, the spacecraft will naturally drift over time and even if the cluster is initialized in such a way to satisfy the distance constraints, sooner or later the relative configuration might become unsafe. The safety of the cluster can be ensured through proper corrective maneuvers, hence the required ΔV can be used as a second key parameter to compare the different techniques.

3.1 Spots versus Spacecraft

For a better understanding of the techniques comparison, a distinction between the spots occupied by the spacecraft and the spacecraft themselves has been made.

The spots are reference locations in which the spacecraft are deployed and which should be tracked. They are directly involved in the search process and are treated as mass-less points. The ultimate goal is to find locations that satisfy the distance constraints indefinitely, so that when the spacecraft are deployed in them and track them through station keeping maneuvers, one can be sure that the distance constraints will not be violated. Due to this distinction, in the early phase of the study, for each set [TIC D_{min} D_{max}], the TIC is used to identify spots that ensure satisfaction of the distance constraints. Once the spots that meet these constraints have been established, they are occupied by the spacecraft, and their subsequent motion is studied.

3.2 Number of Spots

For each set [TIC D_{min} D_{max}] a certain number of candidate spots $n_{s,c}$ is obtained with the initial state of each spot defined as such:

$$\boldsymbol{\alpha}_s(t_0) = f(\boldsymbol{\alpha}_{VP}(t_0), \Delta_s(\text{TIC})) \tag{21}$$

where $s = 1, 2, ..., n_{s,c}$. The function f specifies that the initial state of the s_{th} spot depends on the initial state of the virtual point $\boldsymbol{\alpha}_{VP}(t_0)$ and on some *differences* $\Delta_s(\text{TIC})$, which are applied to it and in turn depend on the considered TIC. For example, the DeEl technique deals with time shifts ($\Delta_s = \Delta t_s$) and propagates the vector $\boldsymbol{\alpha}_{VP}(t_0)$ in time, while the EIVS technique works with non-singular relative elements ($\Delta_s = \Delta \boldsymbol{\alpha}_s^N$) and adds them directly to the vector $\boldsymbol{\alpha}_{VP}^N(t_0)$.

The expression *candidate spots* has been used because Eq. (21) only refers to the initial time t_0, and a set of states satisfying the constraints at t_0 is not an insurance for the future safety of the cluster. Each technique tries to compensate and accommodate the differential perturbations differently, but these can never be entirely canceled and the state vectors will always slowly drift towards an unsafe configuration. Therefore, for the identification of the spots, an additional step is included in the search process to take also their evolution into account: a desired time frame in which the cluster must remain safe is fixed and the relative motion of the candidate cluster is checked for its entire duration. In particular, after the states of the candidate spots are available, they are converted into Cartesian coordinates and propagated for five orbits, while also incorporating the J_2 effect. The choice for such a short time frame is justified considering that some techniques (EIVS, J2In, BFPa) identify the initial configuration by using simplified models of the relative motion, which become less reliable over time. The decision to include the J_2 perturbation is instead motivated by considering that its effect is the largest one for a LEO. A spacecraft would also be significantly perturbed by its interaction with the atmosphere, but it is worth recalling that in this first phase of the study the focus is on the spots, which can be treated as mass-less points free from the effect of the drag.

Once the Cartesian propagation is completed, the relative distances are recovered and checked. At first the check of the maximum distance from the virtual point is considered and the violating spots are discarded from the solution. Afterwards, the attention shifts towards the minimum distance constraint, whose check takes advantage of the graph theory [2, 12]. It is trivial to state that a spot violating the maximum distance constraint cannot be part of the solution, but if the spots (x,y) violate the minimum distance there is no need to remove them both; rather is it enough to discard only one of them and consequently, two solutions may be used, i.e. one including x without y and another including y without x. However, as the number of violations of the minimum distance constraint increases, it becomes more and more difficult to identify the spots to remove; hence the graph theory is exploited. In particular, a graph can be constructed from all the pairs of spots satisfying the minimum distance constraints, so that the identification of the most populated cluster is the maximum clique problem [6, 33].

For the sake of clarity, let us consider a practical example with five candidate spots all satisfying the constraint on the maximum distance. Suppose instead that a violation of the minimum distance is recorded for the pairs of spots (1, 2), (1, 5), and (2, 3). The graph associated with the problem can be expressed through its adjacency matrix:

$$A = \begin{bmatrix} 0 & 0 & 1 & 1 & 0 \\ 0 & 0 & 0 & 1 & 1 \\ 1 & 0 & 0 & 1 & 1 \\ 1 & 1 & 1 & 0 & 1 \\ 0 & 1 & 1 & 1 & 0 \end{bmatrix}$$

which is a 5x5 symmetric matrix consisting of ones and zeros. In particular, a 0 is placed on the entire diagonal and in all those elements (i, j) representing a violation of the minimum distance constraint between the spot i and the spot j. The rest of the elements are instead filled with a 1. By solving the corresponding maximum clique problem, three maximum cliques can be found:

$$C_1 = \{1\ 3\ 4\} \qquad C_2 = \{2\ 4\ 5\} \qquad C_3 = \{3\ 4\ 5\}$$

This means that given the five candidate spots, the largest safe cluster cannot include more than three of them, and moreover not every three-element combination of the five candidates is acceptable, rather only the combinations C_1, C_2, and C_3.

The combinations of spots obtained from the resolution of the maximum clique problem represent then solutions of the initial configuration problem, and once that they are available the search can be considered concluded. Figure 8 shows how the number of spots varies with the D_{max} for all the techniques examined and for D_{min} fixed at 1 km, 5 km, 9 km, 13 km, and 17 km. As expected, for every TIC, the number of returned spots increases when increasing D_{max}, if the D_{min} is given, and decreases when increasing D_{min}, if the D_{max} is given. The less populated clusters are the ones obtained from the EIVS3, whose trend is always the lowest. Similar results can be obtained through the DBNO technique, while a slight increase in the spots number is achieved with the J2In and DeEl, which behave similarly, with trends very close to each other. A first significant increase is achievable through the use of the EIVS1

and EIVS2, and a second one through the use of the BFPa, which returns the largest spots number in most of the cases. The seven techniques can then be divided into three groups (EIVS3-DBNO-J2In-DeEl, EIVS1-EIVS2, and BFPa), whose separation becomes larger and more easily identifiable when reducing the minimum distance boundary. This behavior depends on the fact that the constraints required by the EIVS1-EIVS2 and the BPFa are less restrictive than those imposed by the other techniques, with the consequence that a larger number of vectors satisfying them can be found.

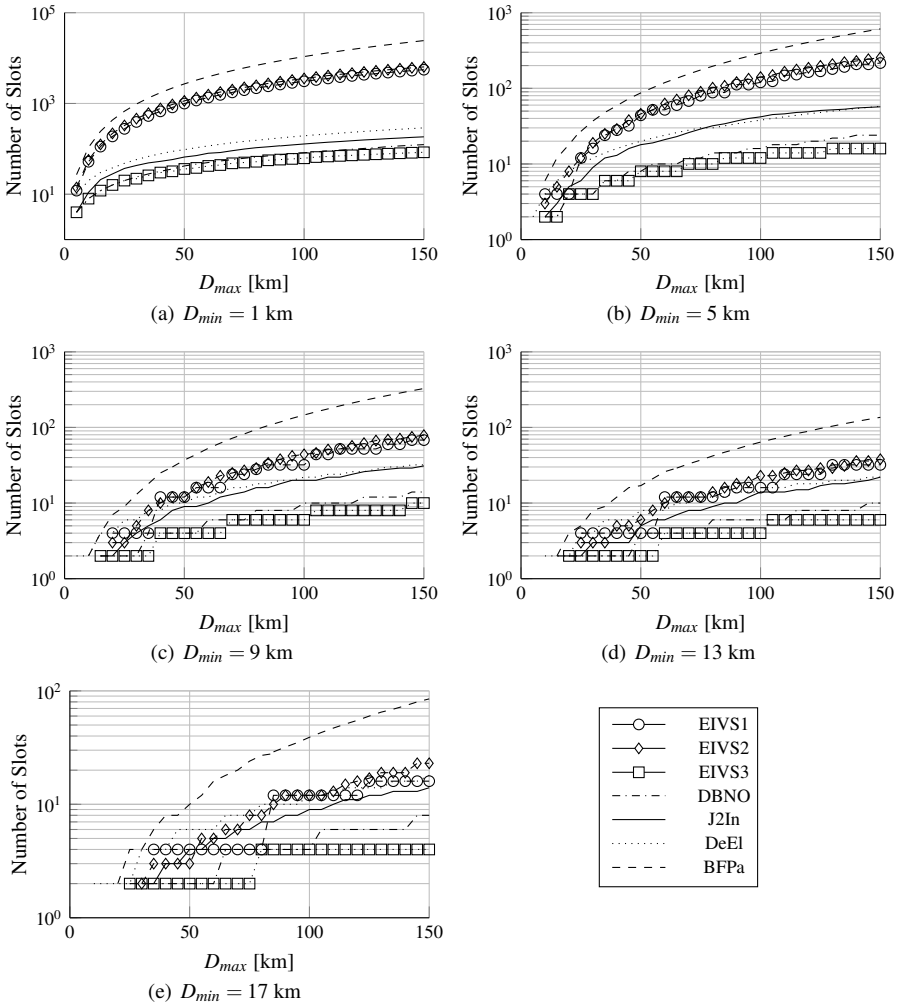

Fig. 8 Number of spots as a function of D_{max} for the different techniques and the different D_{min}.

Graphically Fig. 9 can also help, giving an overview of the arrangement associated with the different techniques. Each subfigure is associated with a TIC and shows

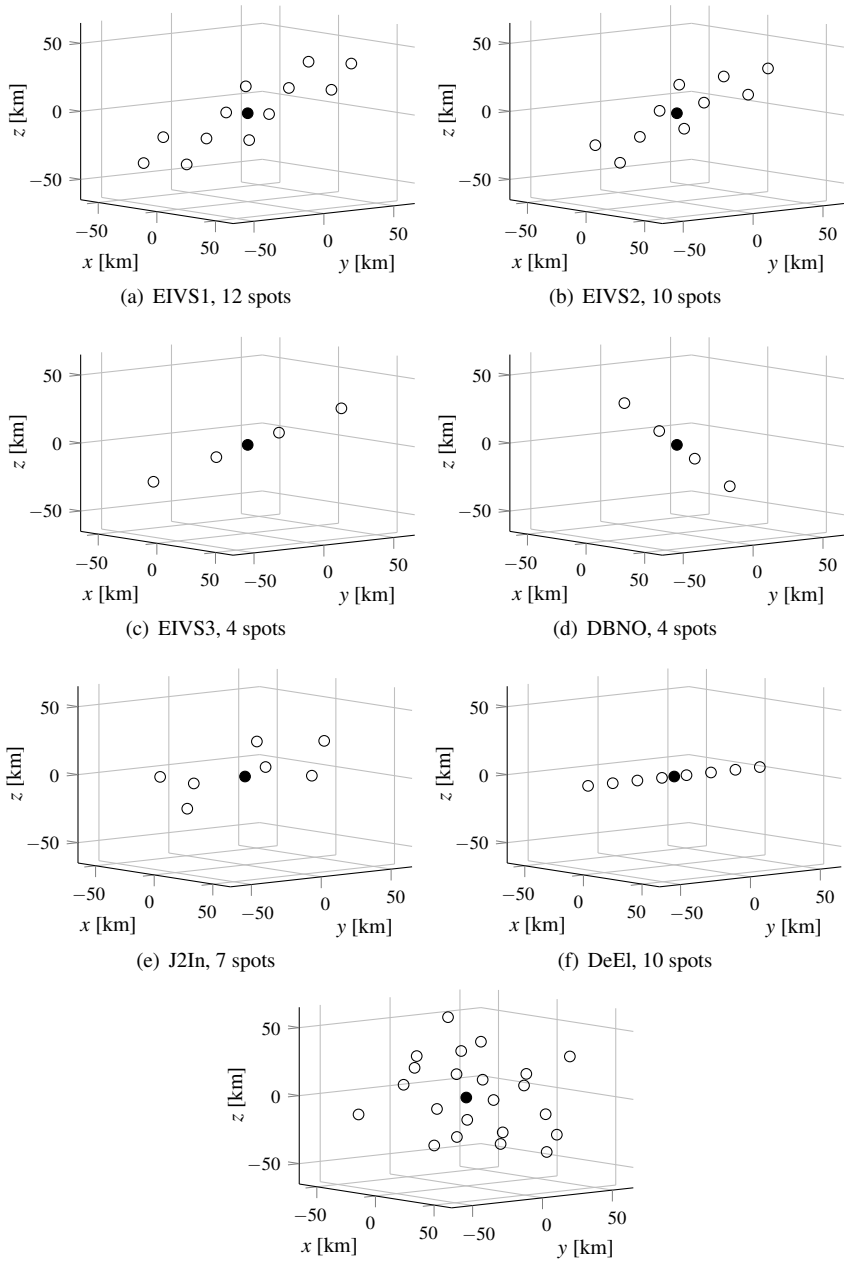

(a) EIVS1, 12 spots

(b) EIVS2, 10 spots

(c) EIVS3, 4 spots

(d) DBNO, 4 spots

(e) J2In, 7 spots

(f) DeEl, 10 spots

(g) BFPa, 28 spots

Fig. 9 Spots arrangements returned by the different TIC: (a) EIVS1, 12 spots (b) EIVS2, 10 spots (c) EIVS3, 4 spots (d) DBNO, 4 spots (e) J2In, 7 spots (f) DeEl, 10 spots (g) BFPa, 28 spots.

the initial configuration of spots around the VP when the distance boundaries are given by $D_R = 17/85$. The representation is given in the LVLH frame centered on the virtual point, which is then located at the center of the subfigures and colored in black. As it can be seen, the spots from J2In and BFPa are distributed in a 3-D region, while the spots from EIVS1 and EIVS2 are densely organized on a plane and the spots from EIVS3, DBNO, and DeEl are arranged on a line.

3.3 Number of spacecraft

After the study of the spots had been completed, the attention has been shifted towards the behavior of the spacecraft, with the final goal of evaluating the ΔV budget required to ensure the distance constraints are satisfied and thus, that the cluster safety is maintained throughout. As a matter of fact, the maximum number of spacecraft that can be packed into a cluster is for sure an important parameter to be considered for a cluster mission, but at the same time one cannot underestimate the key role played by the ΔV budget. To perform this type of analysis, simulations have been run assigning a spacecraft to each spot of a given initial configuration in a direct correspondence manner, so that each spacecraft is assigned to a single spot and aims at tracking it using station keeping maneuvers.

Before specific consideration of ΔV though, an additional intermediate step is required to investigate the number of spacecraft, since this number is not necessarily equal to the number of spots and it can occur that only some spots can host spacecraft. As it can be recalled, every spots configuration had been identified as a solution only if it could satisfy the distance constraints for a time frame of five orbits under the J_2 disturbance. If the spacecraft of the cluster were only perturbed by the J_2 term, a regular cycle of corrective maneuvers performed every five orbits could be set, because the same conditions used for the configuration design would hold. Therefore, each spacecraft would move exactly as its reference spot does and the cluster would be safe for at least five orbits. On the contrary, if the same cluster was studied under a different set of conditions, its safety would not be ensured because the spacecraft trajectories would evolve differently over time and violations of the distance constraints could appear already within the given time frame. When this happens, it can be decided to properly modify the current configuration, or to simply discard it and determine a new one. The first option involves removing the spacecraft which violate the constraints and obtaining a cluster out of a reduced version of the original configuration. In the second case, a brand new search process is involved to find a new safe configuration of spots under the new set of conditions. In this study the first method has been implemented, because in this way it is possible to see how a predefined configuration should be modified according to the changes introduced in the design conditions.

In the performed investigation the new sets of conditions differ from the design ones in respect to the model describing the motion of the spacecraft and to the safety time frame considered. In particular, the environmental model includes terms up to J_{20} of the gravitational potential, as well as drag, in order to have a more realistic scenario. Concerning the time frame instead, the constraints verification has not been

performed only with the five orbits one, rather also time frames of 10 and 15 orbits have been used. This choice permits the observation of two effects associated with a time frame increase: a reduction in the spacecraft number and a reduction in the required station keeping maneuvers. If the time frame increases, the drift of a spacecraft from its initial condition increases as well, and this in turn increases the probability that a violation of the constraints occurs. As a consequence, it is expected that the number of spacecraft within the cluster will decrease, which in turn means that less maneuvers can be performed; thus, each maneuver must compensate for a larger drift.

For this study, five sample configurations have been observed, one for each value of the D_{min} parameter. The constraints for the maximum distance are instead built on a value $D_{max} = 5D_{min}$. The results from the study of the number of spacecraft are reported in Table 2, showing the number of spots n_s and the number of spacecraft n_m for the different techniques and their respective time frames.

D_R	Index	EIVS1	EIVS2	EIVS3	DBNO	J2In	DeEl	BFPa
1/5	n_s	12	14	4	4	4	10	27
	$n_{m,5}$	12	14	4	4	4	10	23
	$n_{m,10}$	12	13	4	4	4	10	16
	$n_{m,15}$	12	12	4	4	4	10	11
5/25	n_s	12	12	4	4	6	10	28
	$n_{m,5}$	12	12	4	4	6	10	23
	$n_{m,10}$	12	12	4	4	6	10	15
	$n_{m,15}$	12	12	4	4	6	10	11
9/45	n_s	12	12	4	4	8	10	30
	$n_{m,5}$	12	12	4	4	8	10	21
	$n_{m,10}$	12	12	4	4	8	10	14
	$n_{m,15}$	10	11	4	4	8	10	11
13/65	n_s	12	12	4	4	7	10	29
	$n_{m,5}$	12	12	4	4	7	10	21
	$n_{m,10}$	12	11	4	4	7	10	15
	$n_{m,15}$	8	10	3	4	7	10	13
17/85	n_s	12	10	4	4	7	10	28
	$n_{m,5}$	12	10	4	4	7	10	21
	$n_{m,10}$	8	10	4	4	7	10	17
	$n_{m,15}$	6	9	2	4	7	10	15

Table 2 Number of spots and spacecraft obtainable for five sample cluster configurations.

It can be noticed that in Table 2 the number of spacecraft appears as $n_{m,o}$ with $o \in [5\ 10\ 15]$. Through this notation the parameter o expresses the time frame, in terms of number of orbits, in which the distance constraints are guaranteed to be satisfied by the n_m spacecraft. Additionally, it can be seen that for a given set of $[D_{min}\ D_{max}]$, the more dense the cluster is, the larger the experienced reduction is. For the techniques EIVS3, DBNO, and DeEl that configure the cluster as a train of elements, all the returned spots can be used to deploy spacecraft (except for the single case $[D_{min}\ D_{max}\ o] = [17\ 85\ 15]$ of the EIVS3), since the differential disturbances

are highly reduced. On the contrary, when the cluster expands on a plane (EIVS1, EIVS2) and in a volume (BFPa) the differential disturbances are considerably larger and when the time frame increases, so does the differential drift of the spacecraft from the path of their reference initial states. This translates to higher chances of constraints violation, with the consequence that a larger reduction of the number of spots available for the spacecraft deployment is detected. In this train of thought, an exception is represented by the J2In, since it also distributes the spots in a 3-D region, but due to the double invariance constraints they are subject to highly reduced differential perturbations and the few of them returned do not suffer from any reduction.

3.4 ΔV Budget

Once that the numbers of spots and spacecraft have been retrieved, the attention can be finally moved towards the fuel consumption. The different TIC examined try to counteract the differential perturbations in a different way, hence it is reasonable to expect a different evolution of the spots/spacecraft over time and therefore, a different amount of ΔV required for the station keeping. As already mentioned, indeed for the ΔV analysis of each initial configuration a direct correspondence between spacecraft and spots has been implemented, so that each spacecraft is assigned to a single spot and tries to track it for the entire time frame while using station keeping maneuvers. This choice is based on the assumption that if a set of spots satisfying the distance constraints is available, forcing the spacecraft to track them should be enough to ensure that their relative distances remain within the allowed boundaries. Also, it has been deemed appropriate to perform cluster keeping through station keeping because a proper cluster keeping strategy depends on the specific technique used to define the initial configuration, while a station keeping approach is simple and generic enough to represent a uniform metric for the comparison of the different techniques.

The station keeping can be thought of as composed of three phases: offset evaluation, maneuver computation and maneuver execution. In the first phase, the spacecraft computes the offset, in terms of differential orbital elements, of its current state from its reference state. In the second phase, the maneuver to cancel the offset is computed as a sequence of impulsive control actions aimed at correcting the orbital elements [14, 26]. Finally, in the third phase the maneuver is executed to steer the spacecraft towards its reference spot. The control strategy is based on the Gauss Variational Equations and on the idea of correcting the orbital elements separately, so that when specific elements are corrected at specific locations along the orbit the undesired change on the other elements is minimized [14, 26]. Given the intention of tracking a reference state, it is very useful to have a control approach that can correct specific elements while minimizing the undesired impact on the others, but this advantage has a price. Each spacecraft requires several separate control actions and for their computation it only takes its own offset into account, while the relative motion with respect to the other spacecraft is neglected. As a result, at the end of the maneuver the offset is removed, but during the transfer arcs between the different provided impulses the distance boundaries might be exceeded.

In this framework, it can be noticed that the coordination of the objects inside the cluster is only partial. On one side, as it will be also explained further in the section, several logics have been used to trigger the corrections and all of them are based on the relative motion (they all exploit, directly or indirectly, the violation of the distance constraints). On the other hand though, each spacecraft is treated individually and controlled in an uncoordinated way, considering that the relative motion during a maneuver is not taken into account.

For the ΔV budget investigation, the focus is placed upon the entire set of configurations presented in Table 2. Also, given the interest in evaluating the ΔV which is required by a cluster in nominal conditions, it is supposed that all the spacecraft are always active and able to perform corrective maneuvers. As previously explained in Section 3.3, a configuration allocating $n_{m,o}$ spacecraft is ensured to satisfy the distance constraints for at least a time frame equal to o orbits, hence if a maneuvering cycle is implemented periodically every o orbits, a safe relative motion should be guaranteed. This control logic is briefly denoted as PM, since at regular time intervals all the spacecraft measure their offsets, compute the corrective maneuver required to cancel them and consequently perform the required control actions. In the following, the notation PM_o refers to the study of the station-keeping problem through the PM logic for those configurations listed in Table 2 and characterized by a number of spacecraft equal to $n_{m,o}$.

Let us now observe once again Table 2 and focus on the first line of each horizontal section. These first lines refer to the configurations of the spots and therefore their values are always at least equal to the values of the three lines below. When a spacecraft is placed in every spot, the resulting cluster is the densest possible, but for the BFPa technique violations of the distance constraints occur in a time frame shorter than five orbits. However, if the attention is paid to the DBNO, J2In, and DeEl techniques, no violation is recorded prior to 15 orbits and thus, very large time frames could be used in the PM logic. This suggests that each TIC could use a different time frame for the PM logic and for this reason an alternative control scheme based on the constraints violation is also investigated. The logic is denoted as CV and involves only the spacecraft affected by the violation of the constraints. This means that each spacecraft executes a correction only in reaction to the violation of one of its distance constraints, so that the violation of the maximum and of the minimum distance causes the activation of only one and two spacecraft, respectively.

The PM logic has the advantage that a predefined scheme for the maneuver computation is available, with already known times at which the computation is performed, but clearly this setting requires an a priori analysis of the constraints violations to properly set the time frame for the maneuvering cycle. Conversely, in the CV logic the distance constraints are actively used and only the involved spacecraft actually perform a maneuver, but as it will be seen exploring the results, it can happen that some spacecraft require very sparse but large corrections, that can produce severe violations of the constraints.

One parameter for the evaluation and comparison of the results can be identified in the average ΔV required by the cluster, i.e. the total ΔV required by all the spacecraft averaged with respect to n_m. This choice is suggested considering the fact that

the number of spacecraft changes with the TIC and usually also with the selected maneuver logic, hence the comparison of the total ΔV would make no sense.

Figures 10 and 11 compare the results obtained with four maneuver logics for the initial configuration returned by the technique EIVS2 for $D_R = 1/5$. The considered time horizon is 10 days.

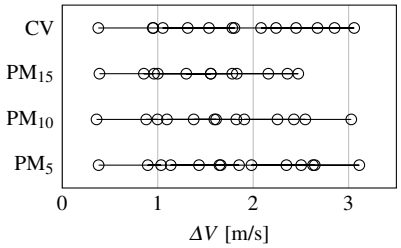

Fig. 10 ΔV budget required by an initial configuration from the technique EIVS2 for four maneuver logics.

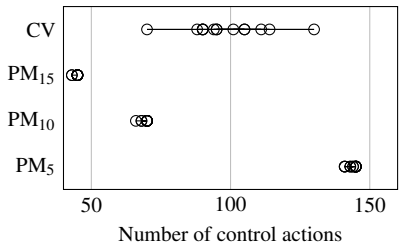

Fig. 11 Number of control actions required by an initial configuration from the technique EIVS2 for four maneuver logics.

In Fig. 10 the ΔV budget is shown, while Fig. 11 gives an overview of the number of required control actions. In both plots a single circle refers to a single spacecraft of the cluster. The spreading of the circles for a given maneuver logic depends on the fact that according to the distance between a spacecraft and the VP, the differential perturbations experienced vary and therefore a different amount of ΔV is required. With particular reference to Fig. 11, when the CV maneuver logic is implemented the differential perturbations cause the spacecraft to violate the distance constraints at varying times, and so the circles are more dispersed. On the other hand, when the PM logic is used, all the spacecraft perform the corrective maneuvers periodically, hence they all require approximately the same number of control actions. It can thus be summarized that for the shown example the maneuver logic does not have a big impact on the average ΔV, rather it affects the number of control actions used and the corresponding impact upon the propulsion system requirements. As a matter of fact, an increase in the time interval between two maneuvers implies larger sparse maneuvers instead of shorter frequent ones.

Table 3 gives instead a measure of the constraints violations recorded in the considered example, showing the minimum and the maximum distances reached. The use of percentage values stems from the comparison of the maximum violations with the foreseen boundaries set at $D_{min} = 1$ km and $D_{max} = 5$ km. The violations of the maximum distance constraints stay below 10% for all the four maneuver schemes, meaning that in all cases the maximum distance reached is up to approximately 10% larger than the 5 km boundary value. The 0% value denotes that no violation occurs. More severe are instead the violations of the minimum distance constraint, since in the worst case the minimum distance reached decreases until 73% of the 1 km boundary value. It must be pointed out that such constraints violations occur sporadically

and always within the first one or two orbits after the execution of the first control action, and as such this does not mean that the station keeping strategy does not work.

	PM_5	PM_{10}	PM_{15}	CV
D_{min}	6.73%	15.00%	26.87%	21.18%
D_{max}	1.22%	9.79%	0%	2.08%

Table 3 Distance violations detected for an initial configuration from the technique EIVS2.

This behavior was anticipated and can be attributed to the particular way the trajectory corrections have been implemented. As a matter of fact, the station keeping is not instantaneous, but is composed of several separate impulsive control actions, taking place at different locations along the orbit. Between the first and the last control action the spacecraft travel on transfer orbit arcs and it is in this short time frame that the violations are recorded. Indeed, as it can be recalled from the description of the three phases of the station keeping, for each spacecraft the required maneuvers are computed to ensure the reference state is tracked, but without taking into consideration the relative motion with respect to the other spacecraft during the execution of the maneuver itself.

Despite the fact that the CV control logic actually requires a violation of the distance boundaries to trigger the computation of a correcting maneuver, in general a violation is clearly undesirable. Nevertheless, in this part of the study the intention was not really to prevent violations as a whole, rather to see if a station keeping approach could be sufficient to perform cluster keeping and to obtain a raw evaluation of the ΔV budget required by different configuration designs.

In Figs. 12 and 13 an overview of the violations is depicted for the constraint of the minimum and of the maximum distance, respectively. Each figure is divided into seven parts in order to compare the different techniques. Each part illustrates the behavior of a TIC through four bars, which correspond to the four tested maneuvering schemes ([a, b, c, d] = [PM_5, PM_{10}, PM_{15}, CV]). Recalling that for a single TIC and a single maneuver logic five sample configurations have been tested, each bar renders the worst out of the five cases, i.e. the largest percentage violation with respect to the reference distance boundary. For example, if one considers the EIVS1 technique and a station keeping strategy applied regularly every five orbits, it can be seen that the maximum violations of the minimum and of the maximum distance constraints are below 10% and 5%, respectively.

Observing the different parts of the two figures individually, in most of the cases the bar height of the PM scheme grows with the maneuvering period. This trend depends on the fact that, as already mentioned, when the time frame between two consecutive maneuvers increases, the differential drift of the spacecraft from the path of their reference states increases as well, so that larger correcting maneuvers are required; thus, larger violations can be experienced. In addition, in the CV cases the bars can become much higher than the PM cases, due to the fact that a maneuver

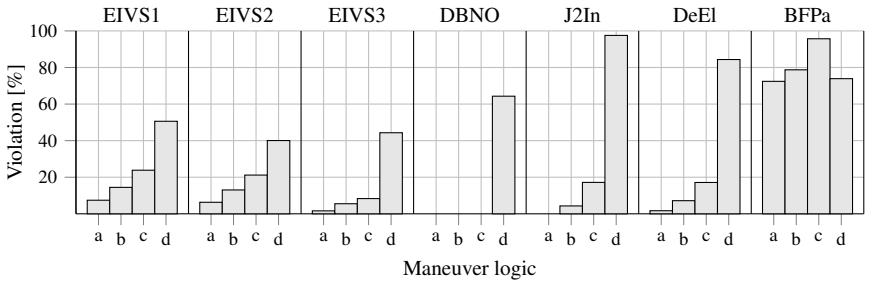

Fig. 12 Violations overview of the minimum distance constraint.

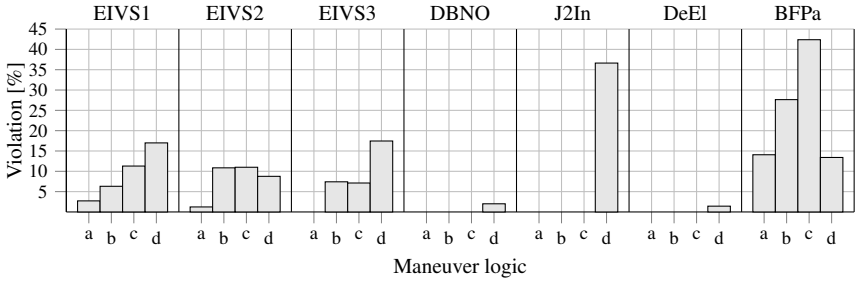

Fig. 13 Violations overview of the maximum distance constraint.

already starts with a violation, which then is accentuated by the application of the corrections.

As a final outcome, it is clear that the station keeping framework is not entirely violation-free and that the relative motion during the transfer paths should also be taken into consideration. If this aspect of the problem was implemented, the control strategy would have been different, consisting of another sequence of control actions but without a substantial change in the overall estimated ΔV budget.

To conclude this part of the study and the comparison of the different techniques, let us now focus on the results of the station keeping investigation in terms of the ΔV required by the spacecraft. To develop this analysis, two points of view can be considered. Let us focus on a single D_R. On one side, one can fix the maneuver logic and pay attention to the entire configurations. From another perspective, it could be interesting to fix a maximum ΔV budget and see, for each TIC, how many spacecraft comply with this limitation. For a better understanding of these two analyses, let us have a look at Figs. 14 and 15, and at Fig. 16, respectively.

Figure 14 focuses on the case $D_R = 1/5$ with station keeping performed every five orbits. Each circle denotes the ΔV required by a spacecraft during the entire time frame of 10 days, while the stars and the solid line connecting them highlight the average ΔV required by the entire cluster. As expected, the less differential perturbations are included in the definition of the initial configuration, the larger the drift among the spacecraft is and the less homogeneous the fuel consumption is. That is why for the DeEl, DBNO, and J2In the ΔV of the single spacecraft are very close to

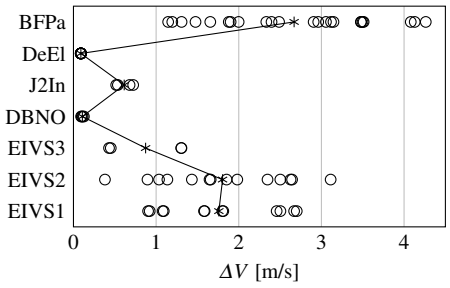

Fig. 14 Station keeping ΔV budget for clusters obtained with different TIC, under equivalent conditions of distance constraints ($D_R = 1/5$) and maneuver logic (PM_5).

the average value, while the fluctuation increases for the EIVS and the BFPa. By assuming that each spacecraft always tracks the same spot, a differential consumption within the cluster was expected. The analysis behind Fig. 14 helps in understanding how penalizing this effect is for the lifetime of the cluster, and also in identifying the spots which, in terms of fuel consumption, are the most expensive.

	EIVS1	EIVS2	EIVS3	DBNO	J2In	DeEl	BFPa
Lifetime Ratio	1.99	7.16	2.03	0.36	0.39	0.06	2.71

Table 4 Comparison of lifetime ratios between most and least expensive spacecraft.

By focusing, for each configuration, on the two spacecraft that consume the most and the least, the ratio of their predicted lifetime can be computed and the results are summarized in Table 4. It can be observed that the differential consumption highly penalizes the EIVS and the BFPa techniques, with the most expensive spacecraft consuming all available fuel up to seven times quicker than the most fuel efficient, and hence cheapest, spacecraft. On the contrary, the reduced differential consumption associated with the DeEl, DBNO, and J2In techniques, translates into a substantial reduction in the spacecraft lifetime differences. Figure 15 gives instead an overview of the distribution of the required ΔV with respect to the position of the spacecraft inside the cluster. The configurations are depicted at the initial time.

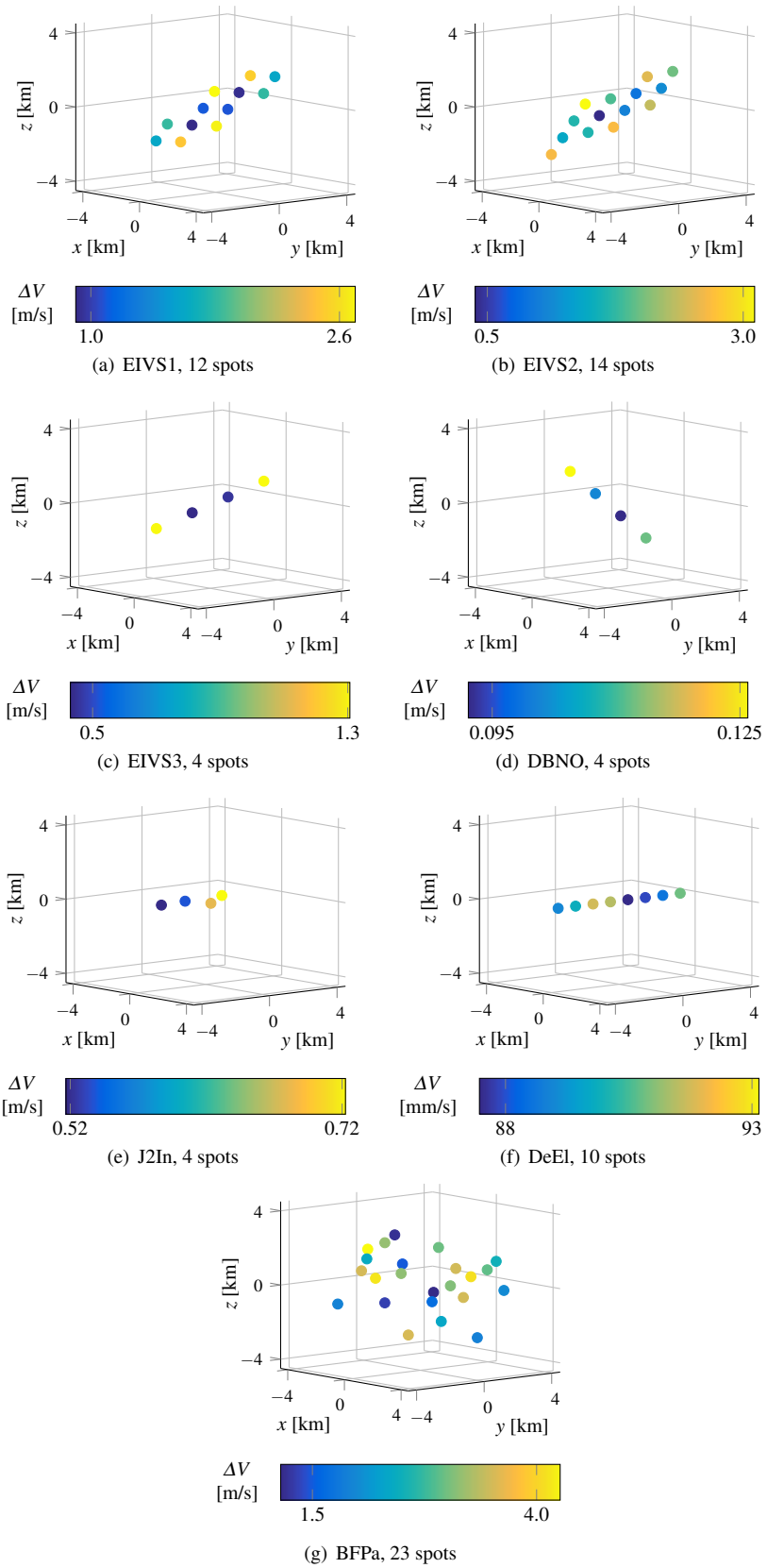

Fig. 15 ΔV distribution for the different positions inside the cluster: (a) EIVS1, 12 spots (b) EIVS2, 14 spots (c) EIVS3, 4 spots (d) DBNO, 4 spots (e) J2In, 4 spots (f) DeEl, 10 spots (g) BFPa, 23 spots.

The second type of research led instead to Fig. 16, which refers again to the case $D_R = 1/5$, but this time all the TIC and the maneuver logics are included. In this analysis it has been identified how many spacecraft could be deployed from the different investigated clusters, when a constraint on the maximum available ΔV is set. For the case given in Fig. 16 five threshold values are considered. It can be observed for example, that if the smallest threshold is selected, only spacecraft consuming less than 0.1 mm/s can be used, which means that only one configuration is available, i.e. a six-objects cluster from the DeEl technique which performs station keeping every five orbits. If the threshold is raised to 1.1 mm/s, solutions from all the other techniques become also available, except for the BFPa. The CV bar of the BFPa does indeed contain a green section, but only one spacecraft can operate with less than 1.1 mm/s of ΔV, and in this situation one cannot refer to *cluster of objects*. To use clusters from the BFPa the maximum allowed ΔV should be set to at least 2.1 mm/s. Similar results are obtained from the other D_R, with the DeEl always demonstrating a good compromise between large number of spacecraft and low ΔV budget, followed by the DBNO and the J2In, and finally by the EIVS and BFPa. In comparison, the EIVS1, EIVS2, and BFPa can always provide the most populated clusters, albeit the price for this asset is paid in terms of high ΔV requirements.

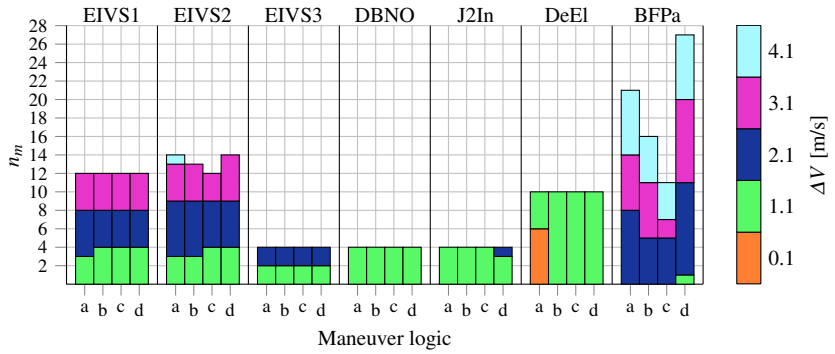

Fig. 16 Number of deployable spacecraft according to different ΔV thresholds for different TIC and different maneuver logics, in the case $D_R = 1/5$.

4 Conclusions

By exploiting the concept of fractionation it is possible to split and replace a single monolithic spacecraft with multiple smaller ones flying in proximity. In such a framework a safe relative motion must be guaranteed, bounding the minimum and the maximum relative distances to prevent collisions and escaping drifts, respectively. With a proper orbit design, the spacecraft might initially satisfy the relative motion constraints, but due to the differential perturbations acting on them, over time their configuration slowly becomes unsafe and corrective maneuvers must be performed. In this work several designs have been surveyed, each providing a cluster

initial configuration while counteracting the differential perturbations with a different approach. The identified test setup assumes that: 1) the cluster is centered on a virtual point; 2) a minimum distance must be ensured between any pair of spacecraft to prevent collisions; 3) a maximum distance must be ensured between any spacecraft and the virtual point to prevent escaping drifts; 4) each spacecraft tracks a reference state through station keeping maneuvers.

In the first part of the investigation, it has been studied how the number of deployable spacecraft changes according to the design technique and to the distance constraints. Every technique ensures indeed a safe relative motion through the satisfaction of a different set of constraints, with the result that the arrangement (and in turn the number) of the spacecraft varies. Concerning the distance constraints, as expected, for every technique the number of deployable spacecraft increases when increasing the maximum distance (if the minimum distance is given) and decreases when increasing the minimum distance (if the maximum distance is given).

In the second part of the research, the obtained initial configurations have been propagated in time and station keeping maneuvers have been implemented to evaluate the ΔV budget required by the single spacecraft and the entire clusters. To start with, the ΔV changes with the design technique, because according to the specific spacecraft distribution, the differential perturbations to counteract vary. Furthermore, a dependency on the distance constraints can also be seen, since the larger the distances are, the larger the differential perturbations to counteract are.

For the study of the ΔV, several station keeping schemes were analyzed, differing from each other mainly by the time span between two consecutive maneuvers and the number of spacecraft involved in each maneuver. In this way it has been possible to observe and analyze two additional aspects of the problem, i.e. the differential consumption of fuel experienced by the spacecraft and the small violations of the distance constraints occurring over time.

Summarizing, from the detailed investigation it emerged that simple station keeping can be a valid option to ensure satisfaction of relative motion constraints among multiple spacecraft. However, in the mission design phase it is not sufficient to choose an initial configuration only according to the desired number of spacecraft and the predicted ΔV budget. Several additional aspects of the problem need to be taken into account, such as the spatial distribution of the spacecraft, the need to introduce countermeasures against violations of distance boundaries, the differential consumption of fuel, etc. All these aspects are clearly interconnected with each other and it is not possible to identify a configuration which has the best performances from all points of view. According to the specific requirements of the mission the best fitting configuration can be different, and that is where the performed study plays its role. This work can indeed provide a helpful tool in order to identify which spots could be used for specific scenarios and moreover, how a safe relative motion can be guaranteed; thus ensuring an effective mission - one in which the safety is not compromised.

Acknowledgements This research has been funded by the German Israeli Foundation Grant No. 1181-220.10.

References

1. Alfriend, K., Vadali, S., Gurfil, P., How, J., Breger, L.: Spacecraft Formation Flying - Dynamics, control and navigation. Butterworth-Heinemann (2009)
2. Balakrishnan, V.: Schaum's Outline of Theory and Problems of Graph Theory. Schaum's Series. McGraw-Hill Education (1997)
3. Battin, R.: An Introduction to the Mathematics and Methods of Astrodynamics, Revised Edition. American Institute of Aeronautics & Astronautics (1999)
4. Beigelman, I., Gurfil, P.: Optimal fuel-balanced impulsive formationkeeping for perturbed spacecraft orbits. Journal of Guidance, Control, and Dynamics **31**(5) (2008). DOI 10.2514/1.34266
5. Bevilacqua, R., Lovell, T.A.: Analytical guidance for spacecraft relative motion under constant thrust using relative orbit elements. Acta Astronautica **102**, 47–61 (2014). DOI http://dx.doi.org/10.1016/j.actaastro.2014.05.004. URL `http://www.sciencedirect.com/science/article/pii/S0094576514001647`
6. Carraghan, R., Pardalos, P.M.: An exact algorithm for the maximum clique problem. Operations Research Letters **9**(6) (1990). DOI 10.1016/0167-6377(90)90057-C
7. Carter, T., Humi, M.: Fuel-optimal rendezvous near a point in general keplerian orbit. Journal of Guidance, Control, and Dynamics **10**(6) (1987). DOI 10.2514/3.20257
8. Clohessy, W., Wiltshire, R.: Terminal guidance system for satellite rendezvous. Journal of the Aerospace Sceinces **27**(9) (1960). DOI 10.2514/8.8704
9. D'Amico, S.: Autonomous formation flying in low earth orbit. Ph.D. thesis, Technical University of Delft, Delft, Netherlands (2010)
10. D'Amico, S., Montenbruck, O.: Proximity operations of formation-flying spacecraft using an eccentricity/inclination vector separation. Journal of Guidance, Control, and Dynamics **29**(3) (2006). DOI 10.2514/1.15114
11. de Bruijn, F.J., Gill, E.: Delayed target tracking for along-track formations. Journal of Guidance, Control, and Dynamics **38**(7) (2015)
12. Diestel, R.: Graph Theory. Electronic library of mathematics. Springer (2000)
13. Eckstein, M., Rajasingh, C., Blumer, P.: Colocation strategy and collision avoidance for the geostationary satellites at 19 degrees west. In: International Symposium on Space Dynamics. Toulouse, France (1989)
14. Fumenti, F., Schlotterer, M., Theil, S.: Quasi-impulsive maneuvers to correct mean orbital elements in leo. In: Proceedings of the 3rd CEAS EuroGNC. Toulouse, France (2015)
15. Fumenti, F., Theil, S.: Advances in Aerospace Guidance, Navigation and Control: Selected Papers of the Fourth CEAS Specialist Conference on Guidance, Navigation and Control Held in Warsaw, Poland, April 2017, chap. Comparison of Multiple Spacecraft Configuration Designs for Coordinated Flight Missions, pp. 585–607. Springer International Publishing (2018). DOI 10.1007/978-3-319-65283-2
16. Gurfil, P., Herscovitz, J., Pariente, M.: The SAMSON project - cluster flight and geolocation with three autonomous nano-satellites. In: 26th AIAA/USU Conference on Small Satellites, SSC12-VII-2. Salt Lake City, UT, USA (2012)
17. Hill, G.: Researches in the lunar theory. American Journal of Mathematics **1**(1) (1878). DOI 10.2307/2369430
18. LoBosco, D., Cameron, G., Golding, R., Wong, T.: The Pleiades fractionated space system architecture and the future of national security space. In: AIAA Space Conference and Exposition, AIAA 2008-7687. American Institute of Aeronautics and Astronautics, San Diego, California (2008)
19. Mazal, L., Gurfil, P.: Cluster flight algorithms for disaggregated satellites. Journal of Guidance, Control, and Dynamics **36**(1) (2013). DOI 10.2514/1.57180
20. Mazal, L., Gurfil, P.: Closed-loop distance-keeping for long-term satellite cluster flight. Acta Astronautica **94**(1) (2014). DOI 10.1016/j.actaastro.2013.08.002
21. Mishne, D.: Formation control of satellites subject to drag variations and J_2 perturbations. Journal of Guidance, Control, and Dynamics **27**(4) (2004). DOI 10.2514/1.11156
22. Montenbruck, O., Kirschner, M., D'Amico, S., Bettadpur, S.: E/I-vector separation for safe switching of the GRACE formation. Aerospace Science and Technology **10**(7) (2006). DOI 10.1016/j.ast.2006.04.001
23. Moreira, A., Krieger, G., Hajnsek, I., Hounam, D., Werner, M., Riegger, S., Settelmeyer, E.: TanDEM-X: a TerraSAR-X add-on satellite for single-pass SAR interferometry. In: International Geoscience and Remote Sensing Symposium, vol. 2 (2004). DOI 10.1109/IGARSS.2004.1368578

24. Persson, S., Jacobsson, B., Gill, E.: PRISMA - demonstration mission for advanced rendezvous and formation flying technologies and sensors. In: 56th International Astronautical Congress, IAC-05-B5.6.B.07. Fukuoka, Japan (2005)
25. Roscoe, C.W.T., Westphal, J.J., Griesbach, J.D., Schaub, H.: Formation establishment and reconfiguration using differential elements in J_2-perturbed orbits. Journal of Guidance, Control, and Dynamics **38**(9) (2015). DOI 10.2514/1.G000999
26. Schaub, H., Alfriend, K.T.: J_2 invariant relative orbits for spacecraft formations. Celestial Mechanics and Dynamical Astronomy **79**(2) (2001). DOI 10.1023/A:1011161811472
27. Schaub, H., Alfriend, K.T.: Hybrid cartesian and orbit element feedback law for formation flying spacecraft. Journal of Guidance, Control, and Dynamics **25**(2) (2002). DOI 10.2514/2.4893
28. Schaub, H., Vadali, S.R., Junkins, J.L., Alfriend, K.T.: Spacecraft formation flying control using mean orbit elements. Journal of the Astronautical Sciences **48**(1) (2000)
29. Tapley, B.D.: Gravity model determination from the GRACE mission. The Journal of the Astronautical Sciences **56**(3) (2008). DOI 10.1007/BF03256553
30. Tschauner, J., Hempel, P.: Rendezvous zu einem in elliptischer bahn um laufenden ziel. Acta Astronautica **11**(5) (1965)
31. Weisstein, E.W.: Cubic close packing. URL `http://mathworld.wolfram.com/CubicClosePacking.html`. From MathWorld - A Wolfram Web Resource
32. Weisstein, E.W.: Hexagonal close packing. URL `http://mathworld.wolfram.com/HexagonalClosePacking.html`. From MathWorld - A Wolfram Web Resource
33. Wood, D.R.: An algorithm for finding a maximum clique in a graph. Operations Research Letters **21**(5) (1997). DOI 10.1016/S0167-6377(97)00054-0
34. Yamanaka, K., Ankersen, F.: New state transition matrix for relative motion on an arbitrary elliptical orbit. Journal of Guidance, Control, and Dynamics **25**(1) (2002)